Chemistry of Metals and Alloys

Chem. Met. Alloys 3 (2010) 161-168
Ivan Franko National University of Lviv
www.chemetal-journal.org

Phase relations along the Ag_8GeS_6–[$(AgBr)_4$·GeS_2] cross-section. Crystal structure and electric conductivity of $Ag_6GeS_4Br_2$ in bulk

Mykola V. MOROZ[1]*, Pavlo Yu. DEMCHENKO[2], Lev G. AKSELRUD[2], Oleksiy G. MYKOLAYCHUK[3], Roman E. GLADYSHEVSKII[2]

[1] *Department of Physics, National University of Water Management and Nature Resources Use, Soborna St., 11, UA-33028 Rivne, Ukraine*
[2] *Department of Inorganic Chemistry, Ivan Franko National University of Lviv, Kyryla i Mefodiya St., 6, UA-79005 Lviv, Ukraine*
[3] *Department for Metal Physics, Ivan Franko National University of Lviv, Kyryla i Mefodiya St., 8, UA-79005 Lviv, Ukraine*
* *Corresponding author. Tel.: +380-36-2235084; e-mail: riv018@i.ua*

Received June 29, 2010; accepted October 29, 2010; available on-line March 2, 2011

The *T*–*x*-diagram of the Ag_8GeS_6–[$(AgBr)_4$·GeS_2] polythermal cross-section has been constructed in the range 25-100 mol.%Ag_8GeS_6. The conditions for solid-state synthesis of the $Ag_6GeS_4Br_2$ quaternary phase have been established. The crystal structure of $Ag_6GeS_4Br_2$ (*Pnma* – d^8c^7a, *oP*96-44.24, Z = 4, a = 6.53892(5), b = 7.72656(5), c = 22.90338(17) Å; X-ray powder diffraction, 820 reflections measured, 58 parameters refined, R_I = 0.0383, R_p = 0.0408, R_{wp} = 0.0528, χ^2 = 1.76) is a disordered variant of the structure determined previously on single crystal data. The electrical conductivity of $Ag_6GeS_4Br_2$ has been measured by the *dc* probe method between 250 and 410 K. A model for the superionic electrical conduction mechanism is proposed.

Ag–Ge–S–Br / Phase diagram / Crystal structure / Electrical conductivity / Superionics

Introduction

The formation of two quaternary phases, Ag_7GeS_5Br and $Ag_6GeS_4Br_2$, has been established in the Ag–Ge–S–Br system. The compound Ag_7GeS_5Br was synthesized by reacting powder mixtures of Ag_2S, GeS_2 and AgBr in vacuum at 973 K [1]. The compound belongs to the family of the mineral argyrodite, space group *F*-43*m*, a = 10.656(4) Å, Z = 4. Information about temperature and composition ranges is limited. The parameters of the conductivity allow assigning Ag_7GeS_5Br to the class of superionic materials [2,3].

Wagener *et al.* [4,5] reported the synthesis by the hydrothermal method and crystal structure (single-crystal data) of the $Ag_6GeS_4Br_2$ compound (space group *Pnma*, a = 6.540(1), b = 7.727(2), c = 22.899(5) Å, Z = 4). The compound is assumed to be metastable at ambient conditions and its thermal decomposition in vacuum occurs at T > 530 K. It was supposed that $Ag_6GeS_4Br_2$ "*…could be obtained up to now by hydrothermal synthesis only and not by conventional solid state reactions…*" [5]. Preliminary measurements of the ionic conductivity using impedance spectroscopy have been made [4]. The compositions Ag_7GeS_5Br and $Ag_6GeS_4Br_2$ lie within the Ag_8GeS_6–[$(AgBr)_4$·GeS_2] cross-section of the quasi-ternary Ag_2S–GeS_2–AgBr system.

The aim of this work was to study the *T*–*x* phase diagram of the Ag_8GeS_6–[$(AgBr)_4$·GeS_2] cross-section near the regions of formation of quaternary phases, synthesize $Ag_6GeS_4Br_2$ by solid-state synthesis, and to determine its crystal structure and electrical bulk properties.

Experimental

The *T*–*x* phase diagram of the Ag_8GeS_6–[$(AgBr)_4$·GeS_2] cross-section was studied using differential thermal analysis (DTA), X-ray powder diffraction (XRPD), and microstructural analysis (MSA). DTA samples were prepared by melting semiconductor grade elemental mixtures in quartz ampoules evacuated to a residual pressure of 1 Pa. The weight of each sample was 0.5 g. The temperatures were determined with accuracy better than ±5 K.

A stoichiometric alloy $Ag_6GeS_4Br_2$ was obtained by a two-temperature synthesis from appropriate amounts of thoroughly mixed Ag_3SBr and GeS_2, or

Ag_3SBr, Ag_2GeS_3 and AgBr powders. Two equal parts of the mixture were placed in the opposite ends of an evacuated ampoule. The synthesis of the alloy was performed in a furnace with a temperature gradient of ~50 K. The temperature of the "hot" zone corresponded to the temperature of peritectic formation of the compound. The alloy was cooled down to room temperature at the rate of ~12-15 K/min after annealing for 2-3 h. The vapor phase condensed in the "cold" zone of the ampoule in the form of a mixture with an undetermined ratio of elemental sulfur, bromine and germanium halogenides. This part of the ampoule with material and condensate was sealed off without depressurization. The next step of the synthesis was performed over 14-16 h at a temperature ~10 K below the temperature of peritectic decomposition of the compound. The equilibrium state of the alloy was achieved under controlled pressure of the gas phase under "dew point" conditions. This method ensured the preservation of the stoichiometric composition $Ag_6GeS_4Br_2$.

XRPD data were collected in the transmission mode on a STOE STADI P diffractometer [6]. A calibration procedure was performed utilizing NIST SRM 640b (Si) [7] and NIST SRM 676 (Al_2O_3) [8] standards. The crystal structure was solved *ab initio*, by direct methods, using WinCSD-2010 [9], and was refined by the Rietveld method [10] with the program FullProf.2k (version 4.60) [11] from the WinPLOTR package [12], applying a pseudo-Voigt profile function and isotropic approximation for the atomic displacement parameters. The crystallographic data were standardized with the program STRUCTURE TIDY [13]. The program DIAMOND [14] was used for structural visualization. More detailed information is given in the supplementary Crystallographic Information File (CIF) (including experimental intensities and structure factors).

The electrical conductivity of $Ag_6GeS_4Br_2$ in the temperature range 250-410 K was measured by the dc probe method in an argon atmosphere at a pressure of ~10^5 Pa. For the measurements we used three types of electrochemical cell (ECC): Ag|alloy|Ag (I), Ag|alloy|Ag_3SBr|Ag (II) and Ag|alloy|Ag_3SI|Ag (III) with Ag|(Ag+Ag_3SBr)|alloy probes, where (Ag+Ag_3SBr) means a well-powdered mechanical mixture of fine-dispersed silver with silver sulfide-bromide. Such a mechanical mixture provides ohmic contact with the alloy. The cells had the form of Teflon bars measuring 10×10×45 mm, with a 2 mm-diameter hole along their length. The constituent components of the cells were pressed into the hole to a density $\rho = (0.93\pm0.02)\rho_0$, where ρ_0 is the crystallographic density of the alloy. The lateral side of the cells had three 0.8 mm-diameter holes in its central part, distant by 5 and 10 mm from each other. These holes were filled under pressure with the probe electrode material. The resistance of the probe contacts was determined by extrapolating the resistance between the probes to zero probe separation. The conductivity measurements were preceded by two heating-cooling cycles in the cells in the temperature range 300-380 K over a period of 5 h. This procedure was intended to eliminate pressing-induced plastic strain. To check the pressing process and assess the effect of electrical and mass transport on the homogeneity of the materials, we used a slightly modified cell IV, similar in configuration to cell I. Its lateral side had a set of Ag|(Ag+Ag_3SBr)|alloy probes throughout the sample length, with a probe separation of 2-4 mm. The length of the alloys in cells I-IV was ~33-35 mm, the thickness of the Ag_3SBr and Ag_3SI layers ~3 mm, and the height of the probe contacts ~2 mm. The silver layer in the electrodes was ~1 mm thick. The cells were connected to the electrical circuit in series. The left-hand electrode had the highest potential. The current through the circuit was $5\cdot10^{-8}$ A, and the input resistance of the voltmeter was above 10^{10} Ω.

The conductivity σ of the alloys was calculated using Ohm's law for a non-uniform portion of the circuit. The calculations were based on the experimental values of the current in the circuit, potential difference, the magnitude and sign of the electromotive force (emf) of polarization between the cell probes as a function of temperature. For each pair of probes in cells (I-III), the $[(\varphi_1-\varphi_2) \pm \varepsilon_{1\text{-}2}] / l_{1\text{-}2}$ ratios (where $\varphi_1-\varphi_2$, $\varepsilon_{1\text{-}2}$ and $l_{1\text{-}2}$ are the potential difference, the polarization emf, and the distance between two arbitrarily chosen probes, respectively) at a given temperature differ by no more than 2-3 %. The discrepancy is concerned with the fluctuation process of electrical and mass transport in the alloy.

Results and discussion

The *T*–*x* space of the Ag_8GeS_6–$[(AgBr)_4 \cdot GeS_2]$ cross-section of the Ag_2S–GeS_2–AgBr system was investigated in the composition range 25-100 mol.% Ag_8GeS_6. Based on the obtained results the phase diagram was constructed (Fig. 1). Two isotherms intersect the section at 676 and 398 K. The isotherm at 676 K corresponds to the formation of a quaternary compound through the peritectic reaction L + HTM-$\overline{Ag_8GeS_6}$ → $Ag_6GeS_4Br_2$ (HTM stands for high-temperature modification; a bar above a compound formula implies a solid solution based on it). The exact composition of this quaternary compound was determined by the Tammann method. A condition for the formation of $Ag_6GeS_4Br_2$ from the melt is that the vapor pressure $p \geq 10^5$ Pa. The compound decomposes below 450 K. This decomposition is due to the decline of the gas-phase pressure, in spite of condensation of its constituents on the container walls. Across the investigated section there is a wide solid solution range HTM-$\overline{Ag_8GeS_6}$ based on the high-temperature modification of the Ag_8GeS_6-phase. The solid solution extends to ~33 mol % $Ag_6GeS_4Br_2$ at 676 K. The region of

HTM-$\overline{Ag_8GeS_6}$ becomes narrower with decreasing temperature. The eutectoid decomposition of the solid solution occurs at the point with the coordinates ~88 mol.% Ag_8GeS_6, T = 398 K (second isotherm in the T–x-diagram). For alloys with composition < 40 mol.% Ag_8GeS_6, reliable data were obtained only for the liquidus line. The slow decomposition of $Ag_6GeS_4Br_2$ and kinetic difficulties connected with the formation of a new set of equilibrium phases at lower temperatures did not allow us to construct the equilibrium phase diagram for this region of T–x-space. According to our investigations, a compound with composition Ag_7GeS_5Br does not form. MSA, DTA and XRPD confirmed the line system of the phase boundary equilibria presented in Fig. 1.

For the high-temperature modification of argyrodite Ag_8GeS_6, a cubic crystal structure of type Ag_8GeTe_6 (space group F-43m, a = 10.7 Å, Z = 4) has been reported [15]. Our XRPD patterns (Fig. 2) show that the crystal structure of HTM-$\overline{Ag_8GeS_6}$ at compositions close to $0.4Ag_8GeS_6$–0.6‘Ag_7GeS_5Br’ can be described in a satisfactory way by the partially disordered model proposed for $Ag_{7-x}GeSe_5I_{1-x}$ (x = 0.31) [16].

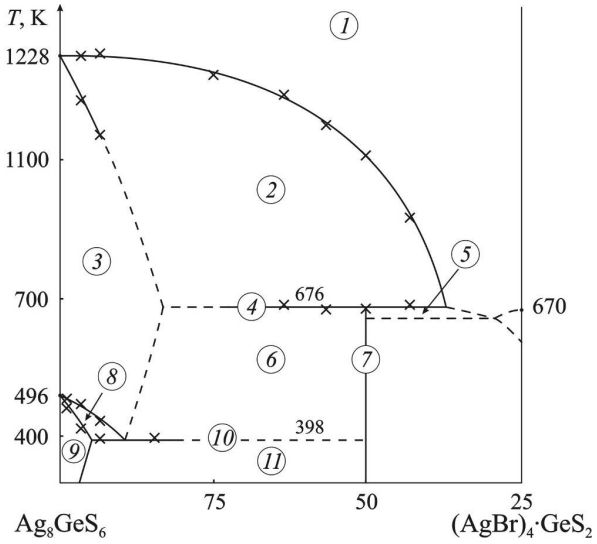

Fig. 1 Ag_8GeS_6–$[(AgBr)_4{\cdot}GeS_2]$ polythermal cross-section in the composition range 25-100 mol.% Ag_8GeS_6: 1 – L, 2 – L + HTM-$\overline{Ag_8GeS_6}$, 3 – HTM-$\overline{Ag_8GeS_6}$, 4 – L + HTM-$\overline{Ag_8GeS_6}$ → $Ag_6GeS_4Br_2$, 5 – L + $Ag_6GeS_4Br_2$, 6 – HTM-$\overline{Ag_8GeS_6}$ + $Ag_6GeS_4Br_2$, 7 – $Ag_6GeS_4Br_2$, 8 – HTM+LTM-$\overline{Ag_8GeS_6}$, 9 – LTM-$\overline{Ag_8GeS_6}$, 10 – HTM+LTM-$\overline{Ag_8GeS_6}$ + $Ag_6GeS_4Br_2$, 11 – LTM-$\overline{Ag_8GeS_6}$ + $Ag_6GeS_4Br_2$. (HTM and LTM are the high-temperature and low-temperature modification, respectively; a bar above a compound formula implies a solid solution based on it).

Crystal data for $Ag_{7.72(4)}GeS_{5.35(3)}Br_{0.844(11)}$: F-43m – h^2e^2dc, cF136-76.38, Z = 4, a = 10.64754(18) Å. 58 reflections measured, 18 parameters refined, R_B = 0.0498, R_p = 0.0608, R_{wp} = 0.0813, χ^2 = 1.82; Cu $K\alpha_1$-radiation. Atomic parameters (x y z, U_{iso} (in Å^2), G): Ge (4d) ¾ ¾ ¾, 0.017, 1; Br (4c) ¼ ¼ ¼, 0.007, 0.844(11); S1 (16e) 0.0260(10) x x, 0.024, 0.336(7); S2 (16e) 0.6258(7) x x, 0.014, 1; Ag1 (48h) 0.0319(2) x 0.2277(2), 0.031, 0.457(4); Ag2 (48h) 0.1132(8) x 0.2756(7), 0.070, 0.186(3).

The investigations show that the solid-state synthesis of $Ag_6GeS_4Br_2$ can be performed in an evacuated (p ~ 1 Pa) quartz ampoule in the temperature region 450-676 K from appropriate quantities of Ag_2S, GeS_2, AgBr (1); Ag_8GeS_6, GeS_2, AgBr (2); or Ag_3SBr, Ag_2GeS_3, AgBr (3). The condition required for the synthesis is the pressure of the gas phase formed by products of decomposition of the initial components and the quaternary phase. The alloy $Ag_6GeS_4Br_2$, obtained under the pressure of the gas phase in equilibrium with the solid phase, was cooled down to room temperature at a rate of ~12-14 K/min. After grinding to a particle size of ≤ 5 μm, the material was dark red-orange in color and was used for XRPD, for conductivity *vs.* temperature measurements, for probe measurements of the distribution of the polarization emf along the length of the pressed alloy in ECC, *etc.* XRPD of the alloys with compositions $0.9Ag_6GeS_4Br_2$–$0.1Ag_8GeS_6$, $0.9Ag_6GeS_4Br_2$–0.1AgBr and $0.9Ag_6GeS_4Br_2$–$0.1GeS_2$ showed two- or multiphase samples and indicated no shifts or intensity changes of the diffraction lines of the $Ag_6GeS_4Br_2$ compound in comparison with the stoichiometric composition. Thus, $Ag_6GeS_4Br_2$ is a compound with constant composition. Refinement of the silver site occupancies (Table 1) yielded the composition $Ag_{5.94(2)}GeS_4Br_2$, in satisfactory agreement with the sample composition.

The crystal structure of bulk $Ag_6GeS_4Br_2$, as found for $Ag_6SnS_4Br_2$ [17], is a disordered variant of the structure reported for $Ag_6GeS_4Br_2$ in [4,5] (single crystal data), derived from it by transfer of some of the silver atoms into interstices, with the formation of defect sites. The arrangement of the germanium (or tin), sulfur, and bromine atoms remains the same in the structures (Table 1, Figs. 3,4, and supplementary CIF).

The distribution of the polarization emf along the alloy length in ECC-IV was studied for the $Ag_6GeS_4Br_2$ compound. It was established that the formation of polarization emf occurs already at the stage of ECC construction (Fig. 5). For the explanation of this phenomenon, we used a model of conduction where the halogen atoms in the crystal structure of $Ag_6GeS_4Br_2$ are assimilated to a quasi-liquid in motion. At the borders electrode-alloy (Ag|alloy) an electrical double layer (EDL) is formed. The formation of EDL is caused by transfer of Ag^+-ions from bulk silver to the investigated alloy

Table 1 Fractional atomic coordinates, equivalent isotropic displacement parameters and site occupancies for $Ag_{5.94(2)}GeS_4Br_2$: *Pnma* – d^8c^7a, *oP*96-44.24, $Z = 4$, $a = 6.53892(5)$, $b = 7.72656(5)$, $c = 22.90338(17)$ Å. 820 reflections measured, 58 parameters refined, $R_B = 0.0383$, $R_p = 0.0408$, $R_{wp} = 0.0528$, $\chi^2 = 1.76$; Cu $K\alpha_1$-radiation.

Site	Wyckoff position	*x*	*y*	*z*	U_{iso} [a] (Å^2)	*G*
Ge	4*c*	0.0043(5)	¼	0.12934(18)	0.0174(10)	1
S1	8*d*	0.3142(7)	0.0117(7)	0.3728(3)	0.0158(16)	1
S2	4*c*	0.1900(12)	¼	0.0484(4)	0.023(3)	1
S3	4*c*	0.2082(11)	¼	0.2038(4)	0.026(3)	1
Br1	4*c*	0.1349(5)	¼	0.70815(15)	0.0248(12)	1
Br2	4*c*	0.1684(5)	¼	0.54072(16)	0.0297(13)	1
Ag1	8*d*	0.0047(9)	0.0646(5)	0.4287(5)	0.0258(10)	0.615(8)
Ag2	8*d*	0.044(3)	0.049(2)	0.4599(14)	0.047(6)	0.145(11)
Ag3	8*d*	0.0525(13)	0.0645(9)	0.2898(4)	0.0298(17)	0.436(11)
Ag4	8*d*	0.1264(10)	0.0224(7)	0.2731(3)	0.0419(18)	0.535(11)
Ag5	8*d*	0.364(9)	0.005(8)	0.492(3)	0.017(13)	0.044(8)
Ag6	8*d*	0.4634(17)	0.0706(11)	0.1065(9)	0.049(4)	0.227(9)
Ag7	8*d*	0.561(2)	0.0440(15)	0.5250(6)	0.036(4)	0.260(10)
Ag8	4*c*	0.4523(9)	¼	0.6258(5)	0.024(2)	0.450(10)
Ag9	4*c*	0.4884(10)	¼	0.6594(4)	0.0376(19)	0.559(10)
Ag10	4*a*	0	0	0	0.026(2)	0.406(12)

[a] For U_{iso} the s.u. obtained in a previous refinement cycle are given. In the final refinement, the site occupancies *G* of the Ag sites were refined for fixed displacement parameters.

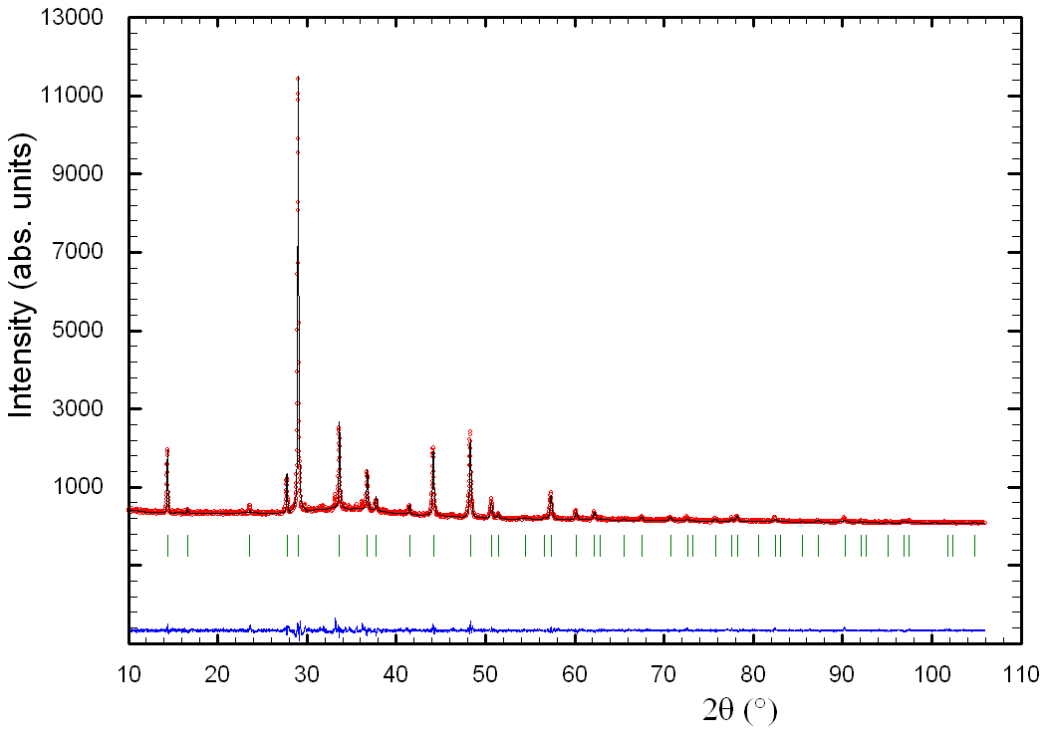

Fig. 2 Observed and calculated X-ray powder profiles for the sample of nominal composition $Ag_{7.4}GeS_{5.4}Br_{0.6}$ (HTM-$\overline{Ag_8GeS_6}$). Experimental data (circles) and calculated profile (solid line through the circles) are presented together with the calculated Bragg positions (vertical ticks) and difference curve (bottom solid line). The sample contains a small amount of low-temperature argyrodite with orthorhombic structure. (Cu $K\alpha_1$ radiation).

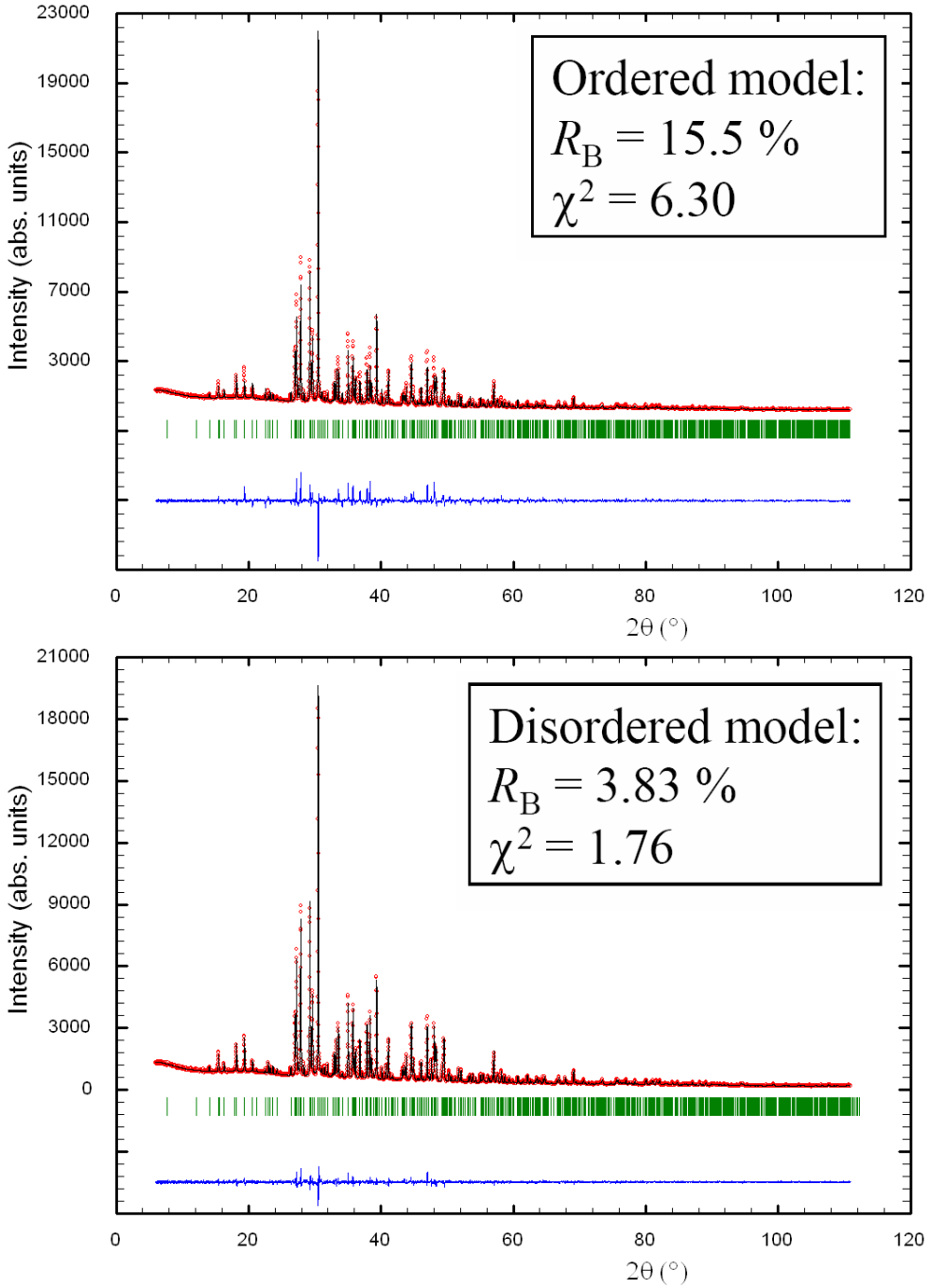

Fig. 3 Observed and calculated X-ray powder profiles for $Ag_6GeS_4Br_2$. Experimental data (circles) and calculated profile (solid line through the circles) are presented together with the calculated Bragg positions (vertical ticks) and difference curve (bottom solid line). Top: ordered model according to [4,5]; Bottom: our disordered model (see Table 1). (Cu $K\alpha_1$ radiation).

due to the chemical potential difference between the contacting materials. This causes a displacement of part of the halogen anions of the pressed alloy towards the electrodes. The excess negative charge concentrates in a narrow field of the investigated alloy, near the electrodes (~5-7 % of their total length). In the central part of the alloy (more than 65 % of the total length) an excess positive charge with a maximum near the middle is formed. The described charge distribution along the alloy length remains infinitely long. This proves that an electronic component of conductivity is absent in $Ag_6GeS_4Br_2$. From Fig. 5, curve 1, an important conclusion can be drawn: the "formula" silver is bound in the cell crystal structure and does not participate in the electrical conductivity process. Curve 2 displays the changes occurring in the structure of the alloy during the charge and mass

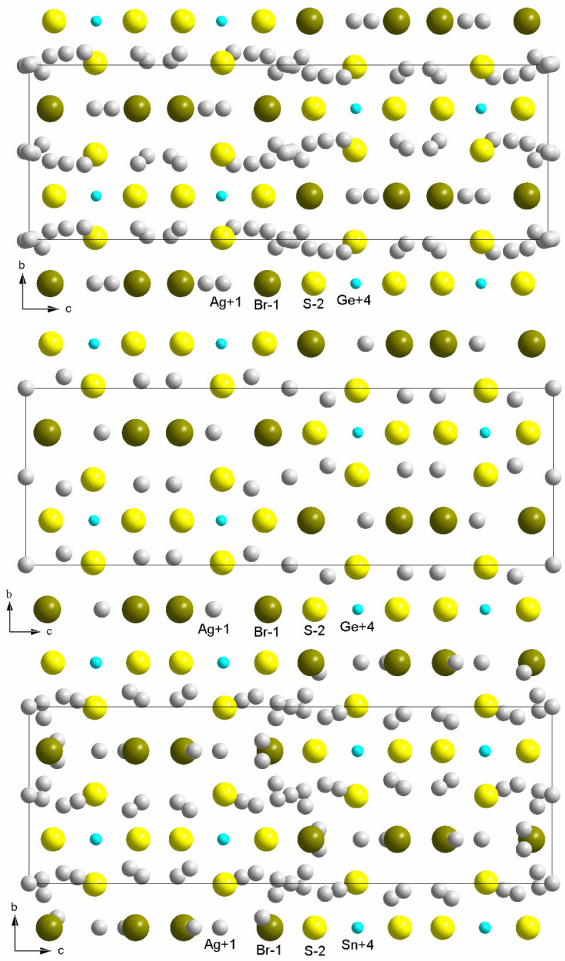

Fig. 4 Comparison of three related structures: bulk $Ag_6GeS_4Br_2$ (this work, top), single crystal $Ag_6GeS_4Br_2$ ([4,5], middle), bulk $Ag_6SnS_4Br_2$ ([17], bottom).

transfer. The electrodes act as sources of silver cations Ag^+ during their transfer through the transport channels. For the halogen anions Br^-, such electrodes are blocking. The halogen anions Br^- drift toward the higher potential electrode (left-hand electrode in the circuit scheme). Supersaturation of ions of both signs in the contact region leads to formation and precipitation of silver halide. The halogen anions that participate in the charge and mass transfer result from alloy electrolysis. The appearance of a second maximum on curve 2 near the right-hand electrode confirms this. In some experiments the compounds Ag_3SBr and Ag_3SI were used as investigated alloy in ECC-IV. It was established that the halogens in these compounds also display the properties of a quasi-liquid in motion [18]. Thus, the layers of ternary compounds that were pressed into the ECC-II and III play the role of source of halogen anions. In such a way, electrolysis of the investigated alloys by the halogen atoms during the studies of their charge and mass transfer was avoided.

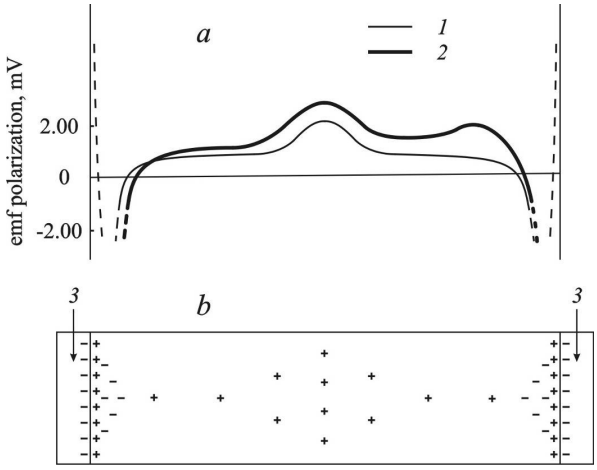

Fig. 5 Distribution of the amplitude of the polarization emf along the $Ag_6GeS_4Br_2$ alloy length at T = 295 K (a): 1 – after one heating-cooling cycle without passing of electrical current, 2 – after two heating-cooling cycles in measuring $\sigma = \sigma(T)$ regime, 3 – the silver electrodes. (b): model for the distribution of electrical charge over the alloy volume for case 1.

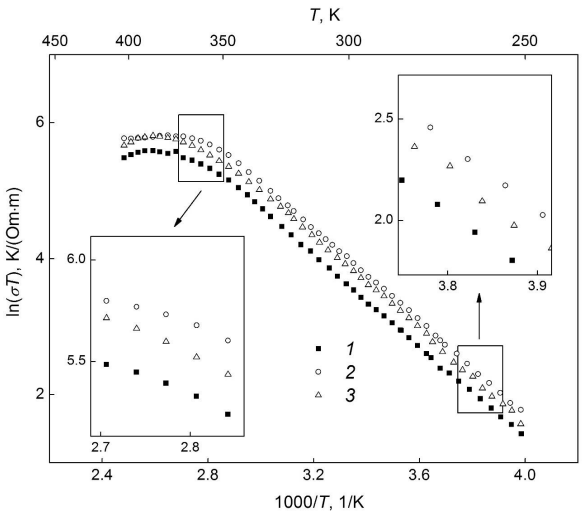

Fig. 6 Temperature dependence of the electrical conductivity of the $Ag_6GeS_4Br_2$ compound in the electrochemical cells ECC-I-III (curves 1-3, respectively).

Fig. 6 displays the temperature dependence of the conductivity of $Ag_6GeS_4Br_2$ in ECC (I-III). The difference in σ between the three ECC is due to the contribution of the anion component (Br^-, I^-) to the conductivity and to the increase of the linear density of halogen atoms along the transport migration channels (ECC-II and III). The change of the linear density of halogen atoms is due to the capture of part of the drift anions Br^-, I^- by structural defects in the transport migration channels (lining the channels).

Table 2 Parameters of electrical conductivity for $Ag_6GeS_4Br_2$.

ECC	Temperature range, K	Analytical equation of temperature-dependent electrical conductivity, K/(Ω·m)	σ, 1/(Ω·m)	
			T = 300 K	T = 340 K
I	260-345	$\sigma T = (2.53\pm0.05)\cdot10^6\exp(-0.288\ \text{eV}/kT)$	0.12	0.40
II		$\sigma T = (4.40\pm0.05)\cdot10^6\exp(-0.293\ \text{eV}/kT)$	0.18	0.59
III		$\sigma T = (2.86\pm0.05)\cdot10^6\exp(-0.299\ \text{eV}/kT)$	0.16	0.54

The mass and charge transfer in the investigated alloy is conveniently described by the model of 'relay mechanism movement' of charge carriers (Ag^+, Br^-, I^-) through the transport migration channels. Such a mechanism was firstly determined by the ^{109}Ag NMR method for the transfer of Ag^+ with the assistance of I^- in $(AgI)_x(Ag_2S{\cdot}GeS_2)_{1-x}$ glasses [19]. Additional information concerning the mechanism of mass and charge transfer is given in [20]. The lining of the transport migration channels by halogen atoms had a positive influence increasing the electrical conductivity of the alloy. The difference between the increase of σ for ECC-II and III is due to the larger size of the iodine anion in comparison with the bromine anion. Reducing the effective cross-section of the transport channels in case of the I^--lining alloy reduces the increase of σ for the material.

In the range 260-345 K, σ measured for $Ag_6GeS_4Br_2$ in the different ECC (I-III) is well described by Arrhenius' equation. The deviation from Arrhenius' law at temperatures higher than 350 K is a result of the decrease of the concentration of charge carriers in the transport migration channels due to the formation of neutral complexes of silver halides. The appearance of a large number of drift charge carriers Br^- in the alloy of ECC-I is associated with the electrolysis of material by the halogen atoms near the right-hand electrode in the circuit scheme. The conductivity values for $Ag_6GeS_4Br_2$ are presented in Table 2. Their magnitude allows assigning $Ag_6GeS_4Br_2$ to the class of superionic materials [21].

Conclusions

The T–x-diagram of the Ag_8GeS_6–[$(AgBr)_4$·GeS_2] polythermal cross-section of the quasi-ternary Ag_2S–GeS_2–AgBr system has been constructed in the concentration range 25-100 mol.% Ag_8GeS_6. The $Ag_6GeS_4Br_2$ compound is formed from the melt at T = 676 K following a peritectic reaction of the liquid with the solid solution HTM-$\overline{Ag_8GeS_6}$. The conditions of the solid-state synthesis of single-phase $Ag_6GeS_4Br_2$ quaternary compound have been established. The formation of an Ag_7GeS_5Br compound was not observed.

The crystal structure of HTM-$\overline{Ag_8GeS_6}$ at concentrations close to the composition 0.4Ag_8GeS_6–0.6'Ag_7GeS_5Br' can be described in a satisfactory way by the partially disordered model of $Ag_{7-x}GeSe_5I_{1-x}$. The crystal structure of $Ag_6GeS_4Br_2$ refined on bulk material ($Pnma$ –d^8c^7a, oP96-44.24, Z = 4, a = 6.53892(5), b = 7.72656(5), c = 22.90338(17) Å; R_I = 0.0383, χ^2 = 1.76) is a disordered variant of the ideal $Ag_6GeS_4Br_2$ structure (single crystal data) and is derived from it by displacement of some of the silver atoms into interstices, with the formation of defect sites.

The electrical conductivity of $Ag_6GeS_4Br_2$ has been measured by a *dc* probe method between 250 and 410 K. The quaternary phase is a purely ionic (Ag^+, Br^-) conductor. Probe measurements of the distribution of the polarization emf along the alloy length showed that the halogen anions in the crystal structure of $Ag_6GeS_4Br_2$ display the properties of a quasi-liquid in motion. The "formula" silver cations are bound in the crystal structure and do not participate in the electrical conductivity process. The electrodes act as a source of drift Ag^+ cations. The conductivity data for $Ag_6GeS_4Br_2$ confirm that this material is a superionic conductor.

References

[1] A. Nagel, K.-J. Range, *Z. Naturforsch. B* 33 (1978) 1461-1464.

[2] M. Laqibi, B. Cros, S. Peytavin, M. Ribes, *Solid State Ionics* 23(1-2) (1987) 21-26.

[3] A. Zerouale, B. Cros, B. Deroide, M. Ribes, *Solid State Ionics* 28-30 (1988) 1317-1319.

[4] M. Wagener, *PhD Thesis*, University of Siegen, 2005, 290 p.

[5] M. Wagener, H.-J. Deiseroth, C. Reiner, *Z. Kristallogr*. 221(5-7) (2006) 533-538.

[6] *Stoe WinXPOW, Version 2.21*, Stoe & Cie GmbH, Darmstadt, 2007.

[7] *SRM 640b: Silicon Powder 2θ/d-Spacing Standard for X-ray Diffraction*, National Institute of Standards and Technology, U.S. Department of Commerce, Gaithersburg, MD, 1987.

[8] *SRM 676: Alumina Internal Standard for Quantitative Analysis by X-ray Powder Diffraction*, National Institute of Standards and Technology, U.S. Department of Commerce, Gaithersburg, MD, 2005.

[9] L.G. Akselrud, P.Y. Zavalii, Yu.N. Grin, V.K. Pecharski, B. Baumgartner, E. Wölfel, *Mater. Sci. Forum* 133-136 (1993) 335-342.

[10] R.A. Young (Ed.), *The Rietveld Method*, *IUCr Monographs of Crystallography N 5*, International Union of Crystallography, Oxford University Press, 1993, 298 p.
[11] J. Rodriguez-Carvajal, *Commission on Powder Diffraction (IUCr), Newsletter* 26 (2001) 12-19.
[12] T. Roisnel, J. Rodriguez-Carvajal, *Mater. Sci. Forum* 378-381 (2001) 118-123.
[13] L.M. Gelato, E. Parthé, *J. Appl. Crystallogr.* 20 (1987) 139-143.
[14] K. Brandenburg, *DIAMOND. Visual Crystal Structure Information System, Version 2.1e*, Crystal Impact, Bonn, Germany, 2001.
[15] O. Gorochov, *Bull. Soc. Chim. Fr.* (1968) 2263-2275.
[16] R. Belin, L. Aldon, A. Zerouale, C. Belin, M. Ribes, *Solid State Sci.* 3 (2001) 251-265.
[17] O.G. Mykolaychuk, N.V. Moroz, P.Yu. Demchenko, L.G. Akselrud, R.E. Gladyshevskii, *Inorg. Mater.* 46(6) (2010) 590-597.
[18] O.G. Mykolaychuk, N.V. Moroz, P.Yu. Demchenko, L.G. Akselrud, R.E. Gladyshevskii, *Inorg. Mater.* 46(7) (2010) 707-710.
[19] J. Roos, D. Brinkmann, M. Mali, A. Pradel, M. Ribes, *Solid State Ionics* 28-30(1) (1988) 710-712.
[20] N.V. Moroz, *Materialy Mezhdunarodnogo Molodezhnogo Nauchnogo Foruma Lomonosov-2010, Podsekciya Fizika Tverdogo Tela*, Moscow State University, 2010 (http://www.lomonosov-msu.ru/archive/Lomonosov_2010/index.htm).
[21] A.K. Ivanov-Shits, I.V. Murin, *Ionika Tverdogo Tela*, Izd. Saint-Petersburg University, 2000, Vol. 1, 616 p.

Proceeding of the XI International Conference on Crystal Chemistry of Intermetallic Compounds, Lviv, May 30 - June 2, 2010.